Catalysis Today 139 (2008) 100–108

Contents lists available at ScienceDirect

Catalysis Today

journal homepage: www.elsevier.com/locate/cattod

Vanadium supported on viscose-based activated carbon fibers modified by oxygen plasma for the SCR of NO

Huacun Huang [a,b], Daiqi Ye [a,*], Bichun Huang [a], Zhengle Wei [a]

[a] College of Environmental Science and Engineering, South China University of Technology, Guangzhou 510006, China
[b] Department of Chemistry and Life Science, Hechi College, Yizhou 546300, China

ARTICLE INFO

Article history:
Available online 25 September 2008

Keywords:
Low temperature SCR
Activated carbon fiber
Vanadium catalyst
X-ray photoelectron spectroscopy
NO

ABSTRACT

Viscose-based activated carbon fibers (VACF) were treated by oxygen plasma modification (OPM) and nitric acid modification (NAM) respectively, and then supported with vanadium oxide. The activities of the catalysts were tested in a laboratory-scale unit measuring significant NO conversions in the selective catalytic reduction (SCR) of NO with NH_3 at low temperature (120–240 °C). The attention was focused on the OPM or NAM on the VACF surface property and the relationship between the surface property and the loading of the vanadium oxide as well as the activities of the catalysts. The textural characteristics were analyzed by SEM, nitrogen adsorption. The surface chemical functional groups were analyzed by X-ray photoelectron spectroscopy (XPS). The results showed that after OPM or NAM, the VACF surface became rougher and a considerable amount of deposition with limited depths appeared on the VACF surface, the average micropore width was slightly enlarged, the pore size distributions of the VACF became wider. XPS revealed that the OPM and NAM could increase the oxygen functional groups on the VACF surface which contributed to a higher vanadium loading and dispersion. OPM or NAM made VACF loaded with vanadium oxide exhibit high activity and made VACF a promising support for SCR at low temperature.

1. Introduction

Many people have attempted to modify the surface properties of activated carbon fibers (ACFs) to improve their functions. The ACF surface modification methods include wet or gas oxidation, plasma treatment, electrochemical oxidation, supercritical fluids, ion or cluster bombardment, etc. Among the oxidation treatments, nitric acid modification (NAM) is the most widely used method to increase the total acidity in a wet oxidation treatment and can be easily controlled by adjusting the concentration and temperature. The carbon materials are sensitive toward the NAM, which gives rise to a large increase in the amount of total acidity resulting from the increase of surface oxide groups such as carboxyl, lactone and phenol. The increase of the total acidity led to an increase of adsorption capacity for metal ions in the whole pH range below the precipitation pH [1]. For example, in the presence of oxygen, the selective catalytic reduction (SCR) activity of a carbon-based briquette catalyst treated with nitric acid at room temperature is promoted by the presence of acidic surface such as carboxyl and lactone, which can help not only to create a reservoir of reactants on the catalysts surface but also to improve the dispersion or even increase the amount of vanadium loading [2]. However, NAM also brings about some problems: (1) reducing the specific surface areas and porosities of ACFs; (2) giving off NO_2 gas during the modification. Most other aqueous oxidants also have similar drawbacks and damage the mesoporous structures at higher temperatures (e.g. >80 °C) [3]. Plasma treatment is regarded as a promising technique for the following reasons. It is a fast solvent-free technique and the operation procedure is simple and can be well controlled. It is also easy to create any ambiance for oxidative, reductive, or inactive reactions by changing the feed gas. It can also produce chemically active species on the ACF surface to affect their functions without changing their bulk properties significantly [4–9]. For example, the CF_4 plasma treatment can effectively improve the hydrophobic property, polarization and power density of the ACFs [10]; the activation of the C-surface by the nitrogen radio frequency plasma yields a significant increase in adhesion for Cu-coatings [11]; the submicron vapour grown carbon fibers preserve their general smoothness upon plasma oxidation and the structural changes brought about by this treatment

* Corresponding author. Tel.: +86 2039380518; fax: +86 2039380518.
E-mail address: cedqye@scut.edu.cn (D. Ye).

0920-5861/$ – see front matter © 2008 Elsevier B.V. All rights reserved.
doi:10.1016/j.cattod.2008.08.028

essentially take place only at the atomic scale [12]; the vapour grown carbon fibers is modified using NH_3, O_2, CO_2, H_2O and HCOOH plasma gases to increase the wettability and the results show that the gases differ in oxidation strength [13]; the polyacrylonitrile fibers are treated with the nitrogen glow-discharge plasma and the hydrophilic groups are introduced on the fiber surfaces [14]; the air and nitrogen glow discharge are used to modify the ACFs, the ACFs surface become rough and several types of polar oxygen groups are introduced into the carbon fiber surface [15].

Recently selective catalytic reduction in the presence of ammonia has become lately the most outstanding technology, and perhaps the most effective one, for the removal of nitrogen oxides [16]. Carbon has attracted much attention as support of transition metal oxides for SCR of NO with NH_3 at lower temperatures, i.e. 100–250 °C [17]. In this way, SCR unit could be located at the downstream of the desulfurizer and/or the particulate control device, at which the temperature is in the range of 120–250 °C [16,18,19].

Up to now, few literatures dealt with the characterization of the structures of vanadium supported on viscose-based activated carbon fibers (VACF). In despite that this catalyst has shown very good performance for the SCR of NOx at low temperature [20]. In this work, the catalytic behaviors of the V_2O_5/VACF catalysts are studied for the SCR reaction at low temperatures. The objective is first the identification of the oxygen plasma modification (OPM) that may lead to higher vanadium loading and higher conversion in the SCR of NO, the especial attention is focused on the effects of preparation parameters of OPM on the VACF surface property and, secondly, studying the relationship between the surface chemistry, porosity and catalytic performance. Herein, VACF have been treated by NAM comparatively.

The VACF have been characterized chemically and texturally. The surface structure of the samples has been characterized by several techniques, viz. SEM and nitrogen adsorption. The surface chemistry has been characterized by X-ray photoelectron spectroscopy (XPS).

2. Experimental

2.1. Materials

The VACF were purchased from Nantong Sutong Carbon Fiber Co., Ltd. (Jiangsu, China). The VACF were initially dried at 130 °C for 10 h to remove the adsorbed moisture.

2.2. OPM and NAM

The experimental apparatus for the NPM is shown in Fig. 1. The dielectric-barrier discharge (DBD) plasma reactor of plate–plate type has a plate size of 180 mm × 60 mm, with barrier thickness of 2.0 mm. The barrier-to-barrier gap between the electrodes was 8.0 mm. Epoxy resin is used for the barrier materials and copper grid for the electrodes. The plasma is generated at a discharge voltage (V) of 6–17.8 kV and a frequency of 50 Hz with a booster (Tengen Group Co., Ltd.) and a transformer. The power consumption (P) in the reactor was approximately 2–20 W measured by a Digital Power Meter (Everfine Instrument Co., Ltd. China) with two high-voltage probes (HVP-40 Max 40 kVdc 28 kVrms). The value of the resistance (R) was 235.0 kΩ. During the plasma treatment oxygen gas was introduced into the reactor at atmospheric pressure. The flow was controlled by mass flow controllers (MFC). The oxygen gas flow rate was 8 ml min^{-1}. The detailed experimental parameters of the different samples are listed in Table 1.

The NAM of the VACF was carried out for 2 h under stirring with HNO_3 (40%, w/w) at 90 °C. Subsequently, the VACF were thoroughly rinsed with distilled water and dried at 130 °C overnight to remove the adsorbed moisture. Vanadium has been supported on VACF with five different loading, viz. 3, 5, 7, 9 and 12 wt.%. The supported catalyst was prepared by pore volume impregnation of the modified VACF with an aqueous solution of ammonium metavanadate (NH_4VO_3). To facilitate the dilution of ammonium metavanadate, ca. 10 mg of oxalic acid was added.

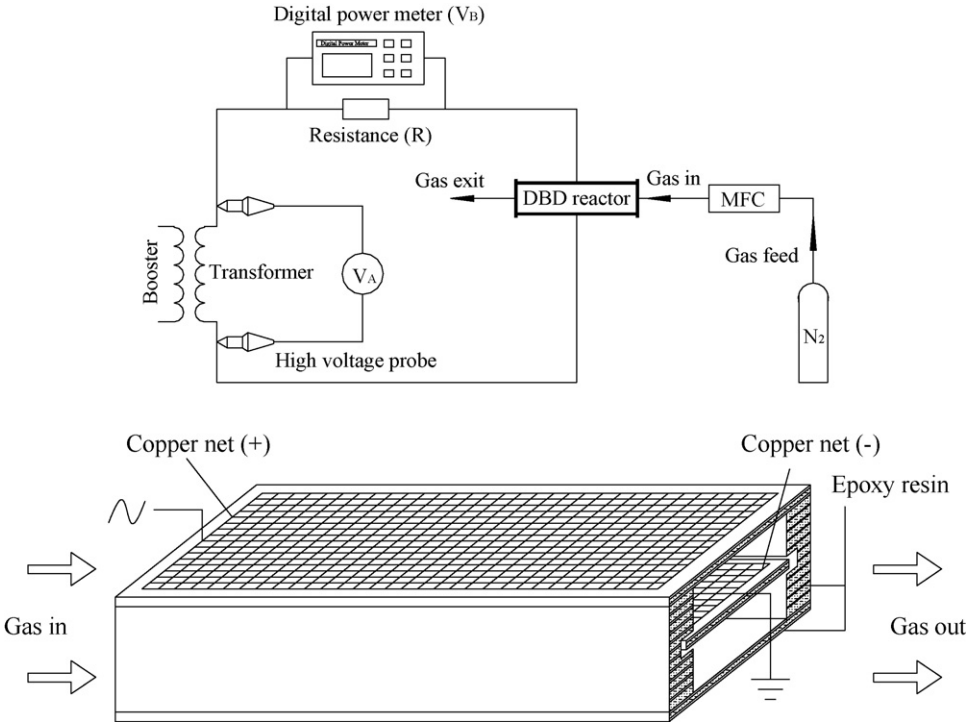

Fig. 1. (a) Schematic of the experimental setup for the DBD plasma treatment and (b) simplified structure of the DBD reactor.

Table 1
Experimental parameters of different samples

Sample code	υ_A (kV)	T[a] (min)	υ_B (V)	I[b] (A)	P[c] (W)
VACF0	0	0	0	0	0
VACF/OPM/10KV-*t*M	10	*t*[d]	145.6	0.62	6.11
VACF/OPM/6KV-40M	6	40	78.5	0.33	1.98
VACF/OPM/13KV-40M	13	40	176.8	0.75	9.65

[a] T: treatment time.
[b] I: electric current in the DBD reactor, $I = \upsilon_B/R$.
[c] $P = (\upsilon_A - \upsilon_B)I$.
[d] t = 5, 20, and 40 min.

Under these conditions, the pH of solution remained neutral, and the solution held a yellow color indicative of the presence of υO_2^+ [21]. It was visually observed that the solution turned from yellow to colorless in a few hours indicating that all the vanadium in solution had been adsorbed. After the impregnation, the catalyst was dried at 65 °C overnight and then at 120 °C for 8 h, followed by a calcination in Ar stream at 500 °C for 6 h and pre-oxidized in air at 220 °C for 5 h. The description of the samples and preparation methods are shown in Table 2.

2.3. Catalysts characterization

The surface morphology change of the VACFs after NPM was observed by a scanning electron microscope (SEM, scanning microscope type S-550, HITACHI, Japan). The samples were examined and typical values of voltage and working distance of operation were 10 kV and 4 mm, respectively. The nitrogen adsorption isotherm at 77 K was measured using an automatic gas adsorption apparatus (Micromeritics ASAP 2010). The BET equation was used to obtain the specific surface areas (S_{BET}) and the adsorption average pore width (W_p, 4V/A). The amount of N_2 adsorbed at relative pressures near unity ($P/P^0 = 0.99$) was employed to determine the total pore volume (υ_t). The *t*-Plot theory was employed to calculate the micropore (~2 nm) surface area (S_{mi}), the external surface area (S_e), and micropore volumes (υ_{mi}). The mesopore (2–50 nm) surface area (S_{me}) and the mesopore volumes (υ_{me}) have been determined by using the Barrett–Joyner–Halenda (BJH) method. Density function theory (DFT) was used to analyze the successive pore size distributions (PSD) curves from micropores to macropores (>50 nm). The functional groups present on the surface of the VACF were also analyzed by X-ray photoelectron spectroscopy (Kratos AXis Ultra, DLD). The measurements were performed at South China University of Technology. Fitting of the V2p spectra was essential for determination of oxidation states of V present in the surface. This was done after subtraction of Shirley background using Lorentzian-Gaussian sum function and XPSPEAK 4.1 software. The C 1s electron binding energy corresponding to graphitic carbon was set at 284.6 eV and used as a reference to position the other peaks.

2.4. Activity tests

The catalysts prepared were tested in the SCR of NO with ammonia at five different temperatures, viz., 120, 150, 180, 210 and 240 °C. The gas composition was 1000 ppm NO, 1000 ppm NH_3, 5% O_2, and the balance Ar. The catalytic tests were performed in a fixed-bed quartz reactor (1.2 cm diameter, 2 cm in length) heated by an electric over. The total amount of each sample was ca. 200 mg. The gas flow rates were controlled by mass flow controllers. The total flow rate was 0.365 L min^{-1} STP, and 6.2×10^{-3} s of residence time (GHSV: 9686.8 h^{-1}). The NO concentrations at both the inlet and the outlet of the reactor were continuously analyzed by an on-line Flue Gas Analyser (TH-990S). The N_2O and NO_2 concentrations in the outlet gases were measured continuously by a gas chromatograph with Porapak Q column. The N_2O and NO_2 have not been observed through this low temperature SCR of NO on the V_2O_5/VACF catalysts. The denitrification activity was expressed as the conversion of NO to N_2.

The percentage of NO reduction was calculated as follows:

$$\%\,\text{NO reduction} = 100 \times \frac{C^{i}_{NO} - C_{NO}}{C^{i}_{NO}}$$

where C^{i}_{NO} and C_{NO} is the measured concentrations of NO at the inlet and outlet of the reactor respectively once the steady state is reached.

Finally, activity tests of 24 h of reaction at five different temperatures, viz., 120, 150, 180, 210 and 240 °C were performed in order to evaluate the catalyst behavior over an extended period of time. In these tests, the NO conversions remained without variation.

3. Results and discussion

3.1. SEM

Fig. 2 shows the SEM micrographs of some typical samples. From the micrographs, the diameter of the samples is in the range of microscale, with some grooves in the axial direction. The presence of these grooves is favorable to form structures with a high surface irregularity. The surface of VACF0 is found to be smooth without deposition under a larger magnification. After the OPM or NAM, the fiber surface became rougher and a considerable amount of deposition with limited depths (bright spots in the SEM image) appeared.

The surface morphology of the materials changed after supporting the vanadium oxide. Much bigger particles of the vanadium species (bright areas in the SEM image) can be observed for the VACF0/V12%, which improves that the distribution of the active phase is not completely uniform and, indicates that the supporting process is ineffective. For the VACF/OPM/10KV-40M/V12%, as illustrated in Fig. 2 after vanadium supporting the thick film of the deposits filled the dents, the growth of granules were also observed. The distribution of vanadium particles plated on the

Table 2
Description of the samples and preparation methods

Sample labeling	Description and preparation
VACF0	The original material
VACF/NAM	VACF treated with HNO_3 (40%, w/w) at 90 °C for 2 h
VACF0/υw%	The VACF0 loaded vanadium with w % (w/w). $w = 3, 5, 7, 9,$ and 12
VACF/NAM/υw%	VACF treated with HNO_3 and loaded vanadium with w % (w/w). $w = 3, 5, 7, 9,$ and 12
VACF/OPM/10KV-*t*M	VACF treated with OPM at 10KV for t min. t = 5, 20, and 40
VACF/OPM/*k*KV-40M	VACF treated with OPM at k KV for 40 min. k = 6, 10, and 13
VACF/OPM/10Kυ-40M/υw%	VACF treated with OPM and loaded vanadium with w % (w/w). $w = 3, 5, 7, 9,$ and 12

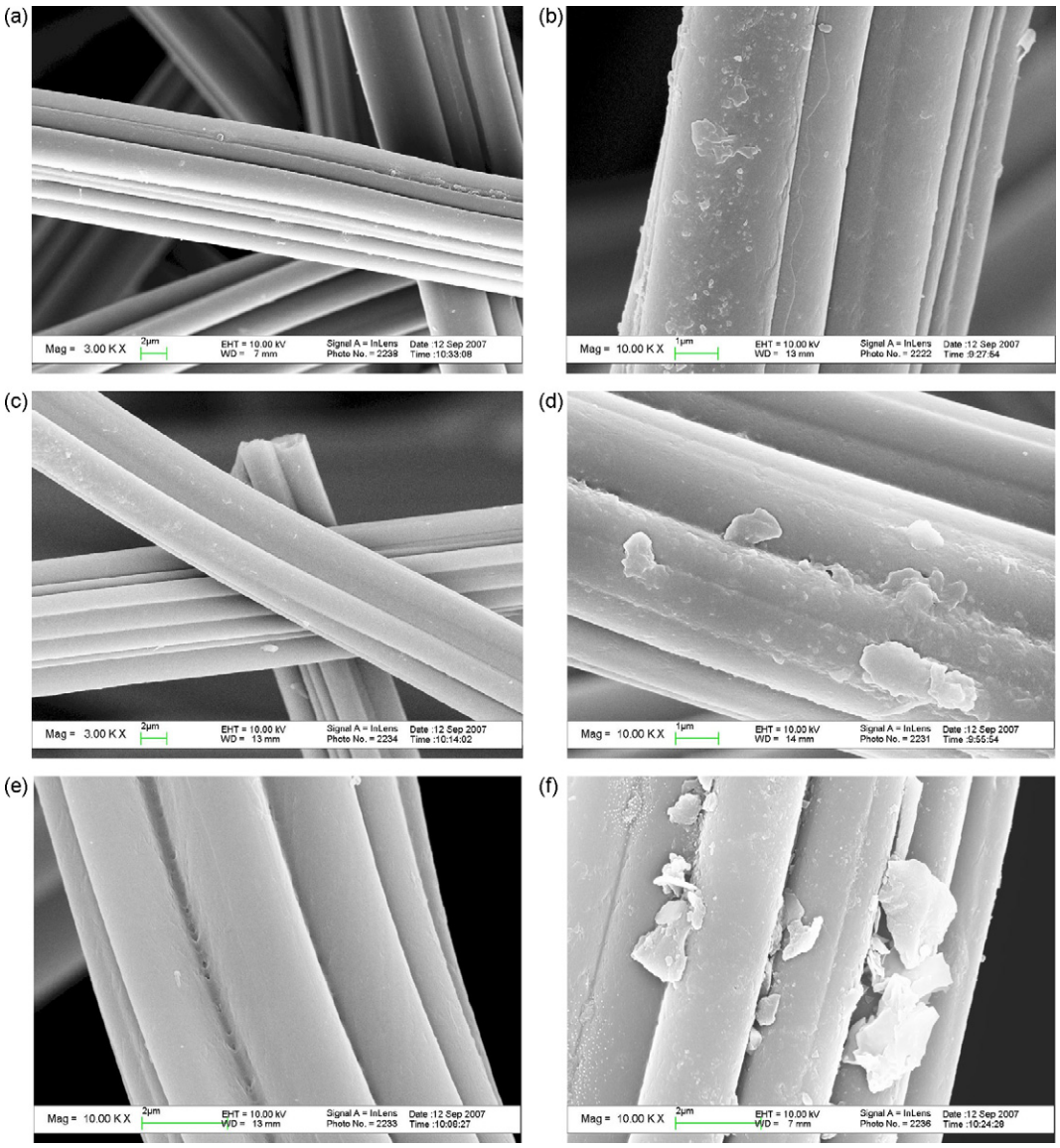

Fig. 2. SEM micrographs of some typical samples: (a) VACF/NAM, (b) VACF/NAM/V12%, (c) VACF/OPM/10KV-40M, (d) VACF/OPM/10KV-40M/V12%, (e) VACF0, and (f) VACF0/V12%.

VACF/NAM/V12% is the most uniform. The thin film on the surface of the VACF/NAM/V12% might be attributed to vanadium species, which is chemically combined with the carbon layer and deposited as monolayer.

XRD measurements (not shown) of these catalysts show no diffraction signal of vanadium compounds even for the VACF0/V12%, which suggests that the vanadium species in the catalysts are in small size and highly dispersed on the VACF surface. It may be associated with the complexity of the VACF surface.

The main result of the OPM and NAM is to obtain a more hydrophilic surface with a relatively large number of oxygen-containing groups (phenol, carbonyl, carboxyl, etc.). The hydroxyl groups in these oxygen-containing groups would enhance the interaction between carbon and vanadium oxide [20] that make highly dispersed V_2O_5 particles in its micropores and large gas contact surface areas. So the higher dispersion has been observed when using VACF supports with a good developed porous structure and with a surface chemistry rich in the more acidic surface groups.

3.2. Nitrogen adsorption

Fig. 3 shows the nitrogen adsorption isotherms for some typical samples. Detailed information on the textural properties of these samples is listed in Table 3.

According to the IUPAC classification [22], the adsorption isotherms of all samples except for the VACF0, VACF/NAM/V5% and VACF/NAM/V12% are of type II, which indicates these samples are the materials with large pores (mesopores and macropores). As shown in Fig. 3(a), the adsorption for N_2 was not yet saturated in spite of $P/P^0 = 1$. The slight gain in uptake at the end ($P/P^0 = 1$) can be attributed to the presence of macropores. The increase of mesopores and macropores might be ascribed to the increasing activation sites or pore widening caused by OPM or NAM, or possibly due to increasing polarity of the samples [23]. The adsorption isotherms of the VACF0, VACF/NAM/V5% and VACF/NAM/V12%, are classified as type I, i.e. the knee of the isotherm is sharp and the plateau is fairly horizontal. This signifies that these samples are microporous ones. It is evident that most of the pore

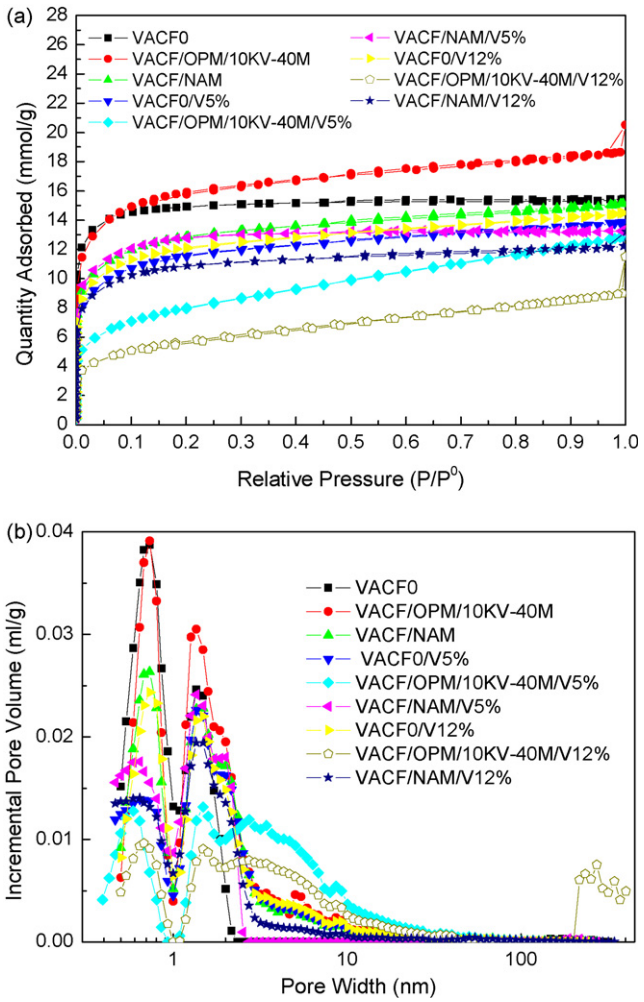

Fig. 3. (a) Nitrogen adsorption isotherms and (b) corresponding PSDs obtained by the DFT of the samples.

volume of these samples is filled below a relative pressure of about 0.1, indicating that these samples are more highly microporous. Nevertheless, there is some contribution of mesoporosity to the total porosity, as indicated by the slight hysteresis of the isotherms.

As shown in Fig. 3(b) and Table 3, for the VACF/OPM/10KV-40M and VACF/NAM, it can be concluded that OPM mainly affect the S_e and the S_{me} while NAM simultaneously affect the S_{mi}, the S_e and the S_{me}. After OPM or NAM, the S_{mi} decreased evidently, the S_e and the S_{me} increased remarkably. NAM made the S_{mi} decrease more evidently than OPM, so the NAM modified the micropore surface more intensively than the OPM. Note that the S_{BET} increased after OPM while the S_{BET} decreased after NAM. The high values of the specific surface area reveal that pore blockage has been avoided to a great extent for the VACF/OPM/10KV-40M. For VACF/NAM, some kind of blockage took place after NAM, but a considerable amount of micropores still remains available. Thus, OPM and NAM can change the pore structure of the samples in a different degree.

As shown in Fig. 3(b) and Table 3, for the VACF0/V5% and VACF0/V12%, after vanadium supporting the υ_t decreased slightly, the υ_{mi} decreased evidently, the S_e, the S_{me} and the W_p increased significantly. The decreasing of the S_{BET} might be due to the following reasons, i.e. the micropore is blocked by the vanadium species or is still closed at the grown of the vanadium species. Because there are less oxygen functional groups on the surface of the unmodified samples that the dispersion of the vanadium species is not good enough and it is easy to produce crystals as shown in Fig. 2. These crystals do not cover the sample surface thoroughly that they do not affect the surface area significantly. The increase of the mesopores or macropores may mainly be caused by other reasons, i.e. the gasification of the VACF during the calcination.

For both VACF/OPM/10KV-40M/V5% and VACF/OPM/10KV-40M/V12%, after vanadium supporting the S_e decreased, the υ_t significantly decreased, the S_{BET}, the S_{mi} and the υ_{mi} reduced most remarkably, and the W_P was widened remarkably. These samples possess primarily mesopores. As shown in Fig. 2, the formation of the thick film of the deposits and the granules should produce a hard coating on the fiber surface, blocking the micropores. Furthermore, the borders of pores correspond to the edges of carbon basal planes where there is a higher density of oxygenated surface groups after OPM that act as anchoring sites for vanadium precursor. Therefore, it is not surprising that the vanadium species are located near the entrance of pores that make the micropore volume reduced [20]. The remarkable decrease in the S_{mi} might suggest that some vanadium be buried in the micropores [24].

For the VACF/NAM/V5% and VACF/NAM/V12%, after vanadium supporting the S_{BET} and the υ_t decreased slightly, the change trend of the S_{mi} is not uncertain, the S_e decreased significantly, the W_p decreased slightly, while intriguingly the S_{me} and υ_{me} decreased most remarkably. So it can be concluded that the vanadium oxide mainly deposited in the mesopore surface for the samples treated with NAM. Compared with the OPM, NAM can modify the internal surface and the external surface at the same time. Because the nitric acid can reach the external and mesopore surface more easily so it is easier to modify the external and mesopore surface, so in the external and mesopore surface there are more oxygen functional groups that can sequester more vanadium oxide after supporting vanadium. This is the reason why the S_{me} and υ_{me} decreased most remarkably. The slightly decrease in the W_p might also suggest that some vanadium might be buried in the mesopores.

Table 3
Pore structure parameters

Samples	S_{BET} ($m^2\ g^{-1}$)	S_{mi} ($m^2\ g^{-1}$) *t*-plot	S_e ($m^2\ g^{-1}$) *t*-plot	S_{me} ($m^2\ g^{-1}$) BJH	υ_t ($ml\ g^{-1}$)	υ_{mi} ($ml\ g^{-1}$) *t*-plot	υ_{me} ($ml\ g^{-1}$) BJH	W_p (Å) BET(4V/A)
VACF0	1124.97	936.03	188.94	75.40	0.53	0.43	0.05	18.98
VACF/OPM/10KV-40M	1224.92	743.44	481.48	250.31	0.64	0.34	0.21	21.05
VACF/NAM	993.16	600.29	392.87	216.84	0.52	0.27	0.18	21.00
VACF0/V5%	900.41	476.76	423.65	216.10	0.48	0.22	0.18	21.22
VACF/OPM/10KV-40M/V5%	635.50	177.29	458.21	335.12	0.44	0.08	0.32	27.82
VACF/NAM/V5%	985.67	632.26	353.41	121.38	0.46	0.29	0.07	18.66
VACF0/V12%	935.46	546.17	389.29	209.09	0.50	0.25	0.18	21.36
VACF/OPM/10KV-40M/V12%	446.48	138.15	308.32	226.57	0.31	0.06	0.21	27.96
VACF/NAM/V12%	835.83	552.28	283.54	141.1	0.42	0.25	0.11	20.28

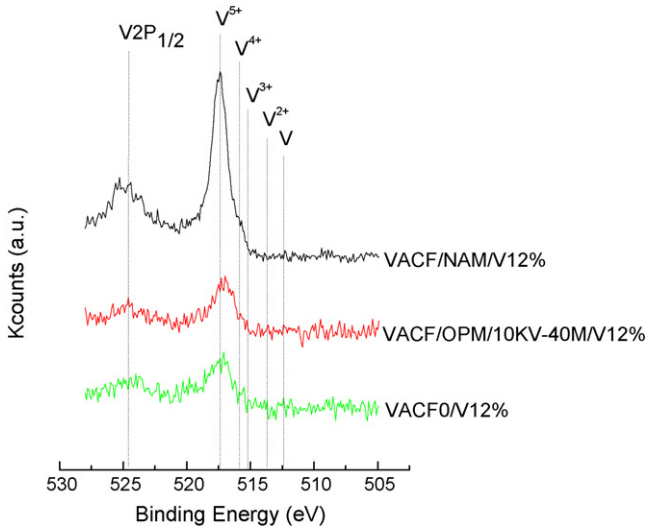

Fig. 4. XPS spectra in the V2p region of V_2O_5, VO_2 and V_2O_3.

3.3. XPS

XPS is applied to estimate the amount of VO_x. Comparison of these values with the data on $V2p_{3/2}$ binding energies for well-ordered vanadium oxide films found in the literature [25,26] allows us to assign the bands at 512.4, 513.6, 515.2, 515.8 and 517.2 eV to V, V^{2+}, V^{3+}, V^{4+} and V^{5+}, respectively. The binding energy of the peak located at 513.6 eV published for thin films of VO. The binding energy of the peak centered at 515.2 eV is in the range of the values reported for bulk V_2O_3 oxides. The binding energies of the peaks located at 515.8 and 517.2 eV are close to those published for bulk VO_2 oxides and bulk V_2O_5 oxides, respectively. Figs. 4 and 5 show the typical XPS spectrums of the VACF0/V12%, VACF/OPM/10KV-40M/V12% and VACF/NAM/V12%. Table 4 summarizes the fractions of V^{5+}, V^{4+} and V^{3+} present in these catalysts. It can be seen that the fractions of V^{5+}, V^{4+} and V^{3+} were slightly different between the original sample and the samples modified by nitric acid or oxygen plasma. It can be observed only the presence of V^{5+} and V^{4+} on the VACF surface after vanadium supporting. The results of the XPS indicate that the predominant species is V_2O_5 oxides. It can be concluded that the VACF support modified by nitric acid or oxygen plasma stabilizes V^{5+} species. Because the V_2O_5 is so active that other more reduced vanadium species form as a consequence of the contact with the other carbon support [16]. This fact was also observed for V_2O_5 loaded VACF.

The C 1s spectra have been resolved into four individual component peaks [27], as illustrated in Fig. 6, namely the following: (1) the graphitic, aromatic, or aliphatic carbon (C–C, 284.6 eV); (2) the ether, phenol or C═N groups (C–O, 285.5 eV); (3) the carbonyl groups (C═O, 287.0 eV); (4) the carboxyl, lactone or esters groups (O═C–O, 288.6 eV). Table 5 shows that after OPM or NAM the graphitic, aromatic, or aliphatic carbon (C–C, 284.6 eV) decrease dramatically especially after NAM. While the phenol, ethers or C═N groups (C–O, 285.5 eV); the carbonyl groups (C═O, 287.0 eV) and the carboxyl, lactone or esters groups (O═C–O, 288.6 eV) increase after OPM or NAM.

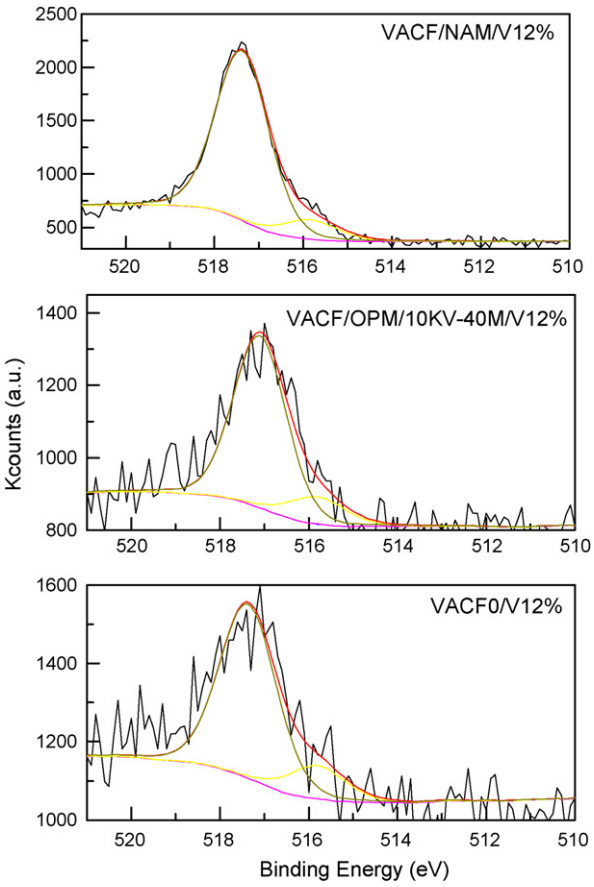

Fig. 5. XPS spectra in the V2p region of V_2O_5, VO_2 and V_2O_3.

Table 5
Relative area (%) of C 1s, XPS for the VACF0, VACF/OPM/10KV-40M and VACF/NAM

Sample	284.6 (eV) C–C	285.5 (eV) C–O	287 (eV) C═O	288.6 (eV) O═C–O
VACF0	83.68	10.48	5.42	0.42
VACF/OPM/10KV-40M	76.66	10.81	9.03	3.50
VACF/NAM	63.08	20.02	11.30	5.60

During the OPM or NAM, surface oxygenated complexes may cause the VACF surface more hydrophilic with a relatively large number of oxygen containing surface groups, and consequently more accessible to the impregnating solution. The surface oxygenated complexes, especially carboxylic acid groups, are also reported to be necessary for the adsorption of cationic precursor [17]. These groups are located in the edges or defects of the basal planes or in the micropores [20]. Accordingly, the vanadium ions will be anchored on these sites. Furthermore, the groups created after the OPM or NAM may contribute to evenly disperse the vanadium.

Table 4
Relative area (%) of V2p, XPS for the VACF0/V12%, VACF/OPM/10KV-40M/V12% and VACF/NAM/V12%

Sample	517.2 (eV) V^{5+}	515.8 (eV) V^{4+}	515.2 (eV) V^{3+}	513.6 (eV) V^{2+}	512.4 (eV) V	Total
VACF0/V12%	83.92	16.05	0.01	0.01	0.01	100
VACF/OPM/10KV-40M/V12%	85.38	14.59	0.01	0.01	0.01	100
VACF/NAM/V12%	89.15	10.84	0.00	0.00	0.00	100

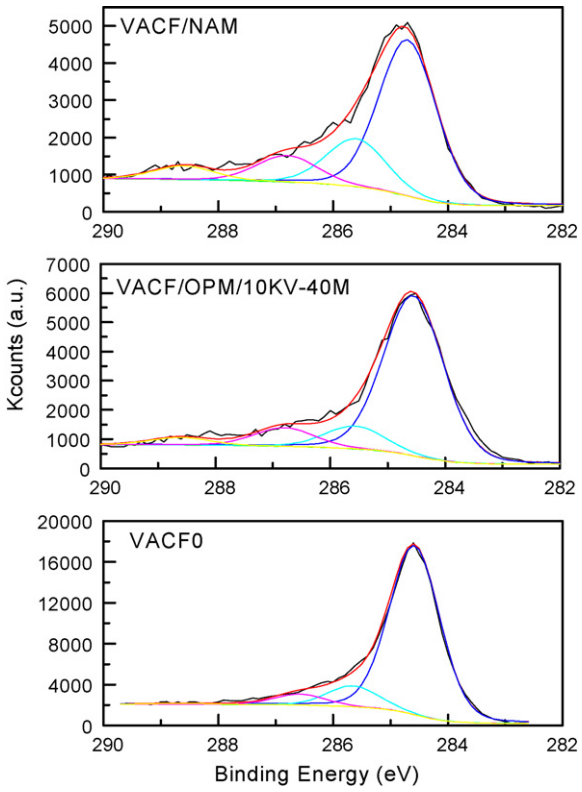

Fig. 6. XPS showing the C 1s core level in VACF0, VACF/OPM/10KV-40M and VACF/NAM.

3.4. Activity tests

Figs. 7–9 shows the effect of reaction temperature on NO conversion at the temperature of 120–240 °C. The NO conversion on the VACF0 and VACF/OPM/10KV-40M increases in the low temperature regime (120–150 °C) and decreases with further temperature increase (150–240 °C). But the NO conversion on the VACF/NAM decreases in the whole temperature range. In contrast, the NO conversion of the samples loaded with vanadium oxide increase with increasing temperature, which corresponds to an activated process. The different activity temperature patterns

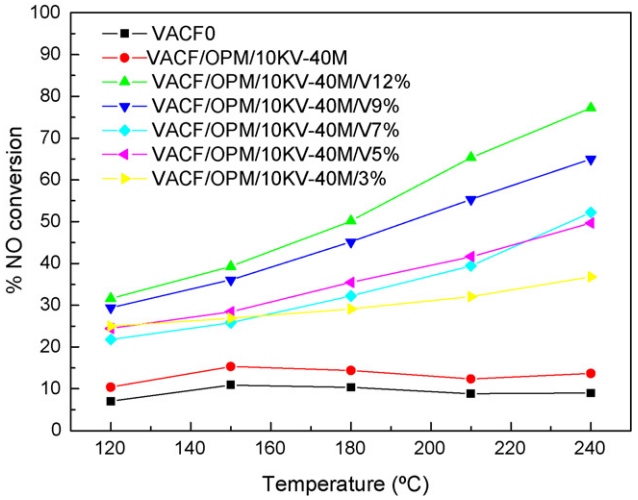

Fig. 8. NO conversion vs. reaction temperature over VACF0, VACF/OPM/10KV-40M and VACF/OPM/10KV − 40M/$\upsilon w\%$ ($w = 3, 5, 7, 9,$ and 12).

indicate that the SCR reaction mechanism on the samples loaded with vanadium oxide is different from that on the unloaded samples. For the unloaded samples, the NO adsorption might be more significant than the catalytic activity.

Figs. 7–9 also shows the activities as a function of V_2O_5 loading. In the temperature range of 120–240 °C, the activities of the VACF unloaded vanadium oxide are very low, with NO conversions of less than 30%. Loading of the vanadium compound leads in all cases to an important enhancement of the activity. As shown in Figs. 7 and 8, an entirely different behavior can be observed, e.g. the vanadium loaded samples show much higher activities than unloaded samples; the activities of the samples loaded with vanadium oxide depend on the V_2O_5 loading, i.e. the activities were directly proportional to the amount at the same reaction temperature. For the catalysts with lower V_2O_5 loading such as 3 and 5 wt.%, their lower activities may be attributed to the lower coverage of vanadium or less number of catalytic sites on the VACF surface.

Fig. 9 shows that for the VACF/NAM/$\upsilon w\%$ ($w = 3, 5, 7,$ and 9) the variation of reduction efficiency with temperature is similar to each other, the change of the loading amount have little or no

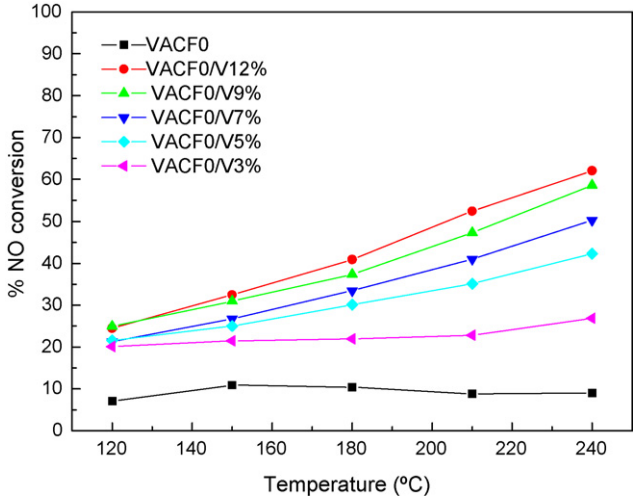

Fig. 7. NO conversion vs. reaction temperature over VACF0 and VACF0/$\upsilon w\%$ ($w = 3, 5, 7, 9,$ and 12).

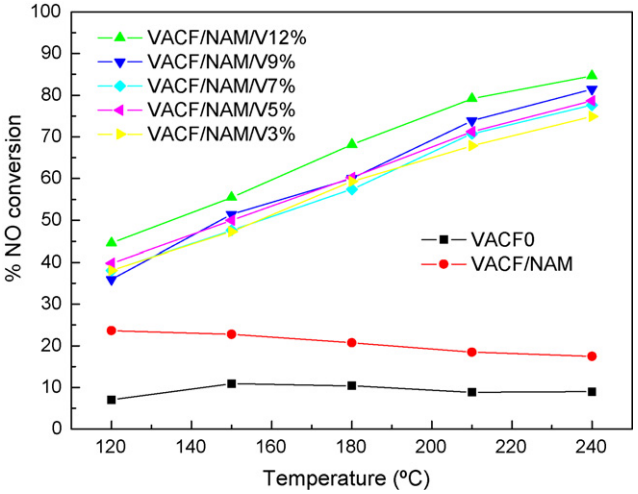

Fig. 9. NO conversion vs. reaction temperature over VACF0, VACF/NAM and VACF/NAM/$\upsilon w\%$ ($w = 3, 5, 7, 9,$ and 12).

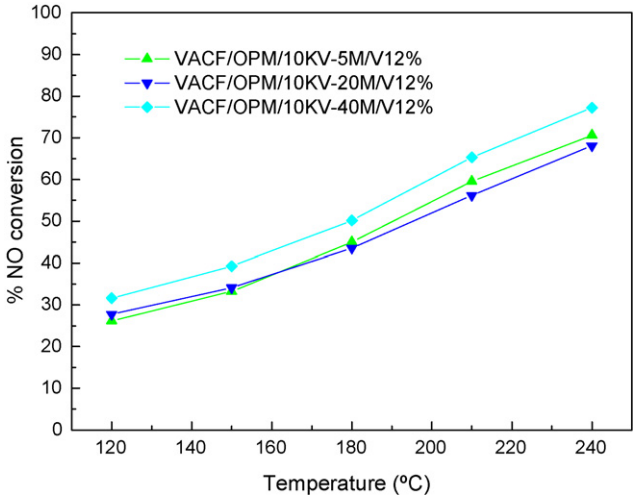

Fig. 10. NO conversion vs. modification time over VACF/OPM/10KV-*t*M/V12% (*t* = 5, 20, and 40).

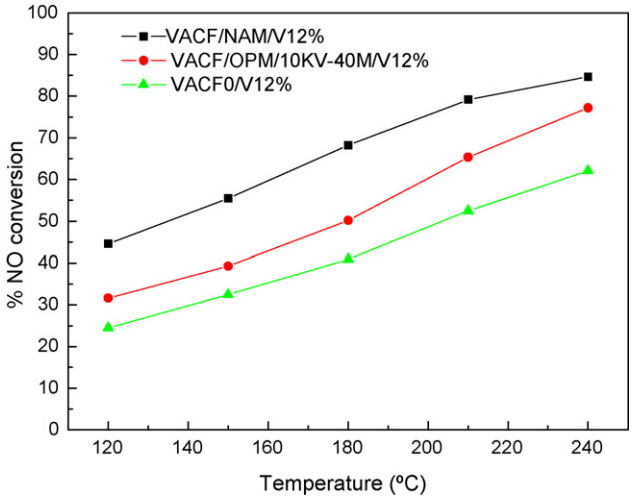

Fig. 12. The effect of VACF pre-treatment on the catalytic activity.

influence on the NO reduction efficiency. But the VACF/NAM/V12% shows the higher efficiency. The NO conversion of the VACF/NAM/$\upsilon w\%$ ($w = 3, 5, 7,$ and 9) are similar indicating that the active sites do not change with the coverage. It is possible that during catalyst calcination a portion of the vanadium species may be reduced by the VACF, and during SCR the reduced vanadium species are gradually oxidized by O_2 (and/or NO) into active vanadium oxide and hence result in increased activity. But for the VACF/NAM/V12% because the reducing substances on the VACF surface is limited that there more active phase produced after catalyst calcination. So the NO conversion of the VACF/NAM/V12% is the highest.

Figs. 10 and 11 show the activities as a function of the treated time and treated voltage, respectively. As shown in Fig. 10 the curves of VACF/OPM/10KV-*t*M/V12% (*t* = 5, 20, 40) present similar appearance. An enhancement of the activity is achieved for VACF/OPM/10KV-40M/V12%. In Fig. 11 the curves of VACF/OPM/*k*KV-20 M/V12% (*k* = 6, 10, 13) also show a similar behavior. So the treated voltage hardly affects the activities. It seems that the treated time can affect the VACF surface properties more intensively than the treated voltage.

The effects of pre-treatment on the catalytic activity are shown in Fig. 12. The NAM and OPM show a positive effect on the activity; the NO conversion of the modified samples are higher than that of the unmodified sample in the whole temperature range; the highest activities are shown by the catalysts pre-treated by NAM. The increased catalytic activity by NAM and OPM possibly result from the increase of oxygen-containing functional groups on the VACF surface, which may have led on one hand to stronger interactions between the vanadium species and the VACF, that may lead to improved dispersion of vanadium species on the VACF surface, and on the other hand they could be favouring ammonia chemisorption acting as reservoir for the reduction reaction. Previous studies [16,28,29] have shown that many activated carbons can sequester metal ions from solutions and metal uptake was assumed to be a function of some surface groups on the carbon, probably –OH functionalities. Thus, the formation of more surface oxygen functional groups as a result of the OPM or NAM may have been responsible for a better distribution of the vanadium over the VACF support, avoiding the agglomeration of particles and the consequent blockage of the pore structure. These agree well with the results of the SEM. As shown in Fig. 2, it is found that VACF/NAM/V12% is more equably covered with vanadium oxide particles after the vanadium supporting. Thus in the case of the samples the catalyst seems to be presented as a thin film, wetting the carbon surface that NO gas can react more actively due to the vanadium oxide nanoparticles, attributed to the specifically increased surface area of the vanadium oxide.

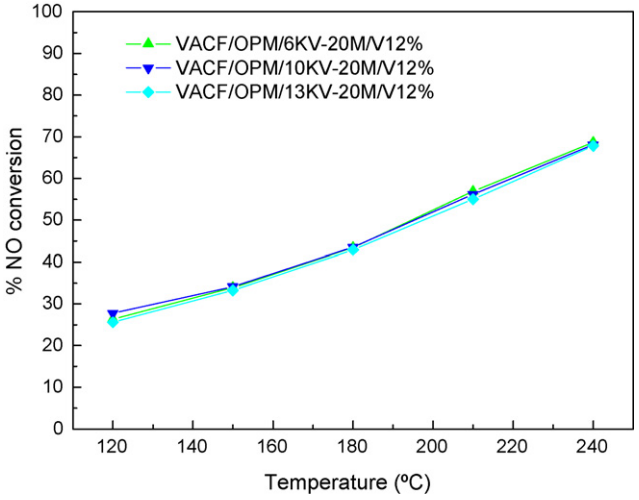

Fig. 11. NO conversion vs. modification voltage over VACF/OPM/*k*KV-20M/V12% (*k* = 6, 10, and 13).

But there is still much confusion concerning the SCR reaction mechanism and the nature of the active centers involved [16], some authors [28,30,31] agree that the low activity of the V_2O_5/VACF catalyst may result from the existence of some reduced vanadium species in the catalysts. This fact is also observed in Table 4 and Fig. 12, e.g. the VACF/NAM/V12% contains less reduced vanadium species, but presents higher NO conversion.

From all the above, the surface features of the VACF played a key role in the vanadium supporting process. The dispersion of vanadium is crucial for the efficiency of the catalyst. The increase of the surface oxygen groups, seem to be crucial for achieving high dispersion catalysts. The achievement of higher dispersion and higher vanadium loadings at monolayer coverage is envisaged as feasible in the VACF support. To meet this objective, the number of oxygen functional groups on the VACF surface can be increased by OPM or NAM. Therefore, the pretreatment with OPM or NAM turn out to be necessary for

impregnation of vanadium. But further research work is needed to optimize the parameters of the OPM.

4. Conclusions

OPM or NAM could make the external surface of the VACF become rougher and a considerable amount of deposition with limited depths appeared on the VACF surface, the average micropore width slightly enlarged, and the PSD of the VACF become wider. XPS revealed that the OPM and NAM could change the distribution of the oxygen functional groups on the VACF surface.

OPM or NAM brought higher vanadium dispersion. It was observed that the carboxylic and hydroxyl surface groups, which increased during OPM or NAM, would enhance the interaction between carbon and vanadium oxide and a more even dispersion of the vanadium species can be clearly obtained. So the previous oxidation of the VACF, concretely using OPM or NAM, led to the production of more active catalyst.

The activity tests show: (1) the NO conversion on the sample loaded with vanadium oxide increases with increasing temperature in the range of 120–240 °C; (2) the NO conversion depends on V_2O_5 loading; (3) the modified time and modified voltage of the OPM do not influence the activity significantly in the conditions tested; (4) both the OPM and NAM show a positive effect on the activity.

OPM or NAM made VACF loaded with vanadium oxide exhibit high activity and made VACF a promising support for SCR of NO at low temperature. But further research work is needed to optimize the parameters of the OPM.

Acknowledgement

This work was partially supported by National Nature Science Foundation of China (20577011).

References

[1] J.W. Shim, S.J. Park, S.K. Ryu, Carbon 39 (2001) 1635.
[2] Doi:10.1016/j.fuel.2007.10.013.
[3] Z.X. Jiang, Y. Liu, X.P. Sun, F.P. Tian, F.X. Sun, C.H. Liang, W. You, C. Han, C. Li, Langmuir 19 (2003) 731.
[4] M.D.G. Domingo-Garcia, F.J. Lopez-Garzon, M. Perez-Mendoza, J. Colloid Interface Sci. 222 (2000) 233.
[5] S. Kodama, H. Habaki, H. Sekiguchi, J. Kawasaki, Thin Solid Films 407 (2002) 151.
[6] H.C. Wen, K. Yang, K.L. Qu, W.F. Wu, C.P. Chou, R.C. Luo, Y.M. Chang, Surf. Coat. Technol. 200 (2006) 3166.
[7] J.P. Boudou, J.I. Paredes, A. Cuesta, A. Martinez-Alonso, J.M.D. Tascon, Carbon 41 (2003) 41.
[8] D. Lee, S.H. Hong, K.H. Paek, W.T. Ju, Surf. Coat. Technol. 200 (2005) 2277.
[9] H.C. Huang, D.Q. Ye, B.C. Huang, Surf. Coat. Technol. 201 (2007) 9533.
[10] Y.H. Pai, J.H. Ke, H.F. Huang, C.M. Lee, J.M. Zen, F.S. Shieu, J. Power Sources 161 (2006) 275.
[11] C. Eisenmenger-Sittner, C. Schrank, E. Neubauer, E. Eiper, J. Keckes, Appl. Surf. Sci. 252 (2006) 5343.
[12] J.I. Paredes, A. Martinez-Alonso, J.M.D. Tascon, Carbon 40 (2002) 1101.
[13] V. Bruser, M. Heintze, W. Brandl, G. Marginean, H. Bubert, Diam. Relat. Mater. 13 (2004) 1177.
[14] Y.C. Liu, D.N. Lu, Plasma Chem. Plasma Process. 26 (2006) 119.
[15] Q. Zhu, J. Sun, C. He, J. Zhang, Q.J. Wang, Macromol. Sci. Pure 43 (2006) 1853.
[16] M.J. Lazaro, M.E. Galvez, C. Ruiz, R. Juan, R. Moliner, Appl. Catal. B 68 (2006) 130.
[17] E. Garcia-Bordeje, M.J. Lazaro, R. Moliner, P.M. Alvarez, V. Gomez-Serrano, J.L.G. Fierro, Carbon 44 (2006) 407.
[18] Z.P. Zhu, Z.Y. Liu, S.J. Liu, H.X. Niu, T.D. Hu, Appl. Catal. B 26 (2000) 25.
[19] Y.L. Wang, Z.Y. Liu, L. Zhan, Z.G. Huang, Q.Y. Liu, J.R. Ma, Chem. Eng. Sci. 59 (2004) 5283.
[20] E. Garcia-Bordeje, M.J. Lazaroa, R. Moliner, J.F. Galindo, J. Sotres, A.M. Baro, Appl. Surf. Sci. 228 (2004) 135.
[21] E. Garcia-Bordeje, L. Calvillo, M.J. Lazaro, R. Moliner, Ind. Eng. Chem. Res. 43 (2004) 4073.
[22] K.S.W. Sing, D.H. Everett, R.A.W. Haul, L. Moscou, R.A. Qierotti, J. Rouquerol, T. Siemieniewska, Pure Appl. Chem. 57 (1985) 603.
[23] J.C. Xie, X.H. Wang, J.Y. Deng, L.X. Zhang, Appl. Surf. Sci. 250 (2005) 152.
[24] E. Garcia-Boudeje, M.J. Lazaro, R. Moliner, J.F. Galindo, J. Sotres, A.M. Baro, J. Catal. 223 (2004) 395.
[25] C. Hess, J. Catal. 248 (2007) 120.
[26] N. Alov, D. Kutsko, I. Spirovovab, Z. Bastl, Surf. Sci. 600 (2006) 1628.
[27] C.L. Mangun, K.R. Benak, J. Economy, K.L. Foster, Carbon 39 (2001) 1809.
[28] Z. Zhu, Z. Liu, S. Liu, H. Niu, Appl. Catal. B 23 (1999) 229.
[29] B.M. Weckhuysen, D.E. Keller, Catal. Today 78 (2003) 25.
[30] E. Hums, Catal. Today 42 (1998) 25.
[31] M.E. Galvez, M.J. Lazaro, R. Moliner, Catal. Today 102/103 (2005) 142.